TRANSACTIONS ON EMERGING TELECOMMUNICATIONS TECHNOLOGIES
Trans. Emerging Tel. Tech. (2013)
Published online in Wiley Online Library (wileyonlinelibrary.com). DOI: 10.1002/ett.2702

RESEARCH ARTICLE

CoPoMo: a context-aware power consumption model for LTE user equipment†

Bjoern Dusza[1]*, Christoph Ide[1], Liang Cheng[2] and Christian Wietfeld[1]

[1] Communication Networks Institute, TU Dortmund University 44227 Dortmund, Germany
[2] Department of Computer Science and Engineering, Lehigh University Bethlehem, PA, USA

ABSTRACT

Increasing the battery lifetime of power-hungry mobile devices has become a major research target for mobile operators. Based on extensive measurement campaigns with the most recent Long Term Evolution (LTE) devices, we introduce a new Markovian power consumption model, which takes into account the chosen system parameters (such as the number of physical resource blocks) as well as the context of a user in terms of radio channel conditions and service characteristics (non-real-time vs. real time). One key advancement of this generic model is its stochastic nature, which allows for determining the average power consumption of a device based on usage profiles including location information and service statistics. We have conducted comprehensive system simulations using realistic channel characteristics derived from ray-tracing analyses and validated the new model. Finally, we show that the proposed context-aware power consumption model enables quantitative analyses of the trade-off between network resource allocation and enhanced battery lifetime.

***Correspondence**
Bjoern Dusza, Communication Networks Institute, TU Dortmund University, Otto-Hahn Str. 6, 44227 Dortmund, Germany.
E-mail: bjoern.dusza@tu-dortmund.de

Received 8 March 2013; Revised 21 May 2013; Accepted 26 July 2013

1. INTRODUCTION

The overall energy efficiency of mobile networks has become a major research focus for designing and implementing the current and next generations of wireless networks. The power consumption of user devices has been an ongoing design issue with solutions such as power management algorithms [1, 2] and dedicated embedded hardware platforms [3]. Recently, the reduction of the power consumption of radio network infrastructure components has also been addressed in the context of green energy deployments and operational expenditures reduction plans [4, 5]. Beyond that, novel applications of cellular networks such as Machine-to-Machine communication pose additional requirements on the energy efficiency of mobile devices [6–8]. Despite these efforts, current smartphones and notebooks still suffer from short battery lifetime when used intensively in mobile networks [9]. In [10], it is emphasised that the battery lifetime of mobile communication devices is one of the most important decision parameters for customers. Mobile operators may actively control and differentiate the battery lifetime of user devices as an adaptable Quality of Experience (QoE) parameter (cf. Figure 1) by deploying network resource allocation strategies based on power consumption models of mobile devices. In this paper, we introduce a new context-aware Markovian power consumption model that enables quantitative analyses of the trade-off between network resource allocation and enhanced battery lifetime.

The accurate modelling and forecasting of the power consumption of embedded devices has recently received increased attention. Table I provides a summary of selected power consumption modelling approaches, which we have classified based on system parameters as well as context parameters. The classification also distinguishes if a parameter was considered as deterministic (marked 'D') or if the model takes into account stochastic characteristics (marked 'S'). The overview shows that the previous work has limitations in addressing only selected deterministic system-dependent and/or context-dependent impacts on the power consumption.

To overcome the limitations of existing models, we introduce, to the best of our knowledge, for the first time, a stochastic *Co*ntext-Aware *Po*wer Consumption *Mo*del (CoPoMo) with multiple LTE system parameters. The key contributions of CoPoMo are the following:

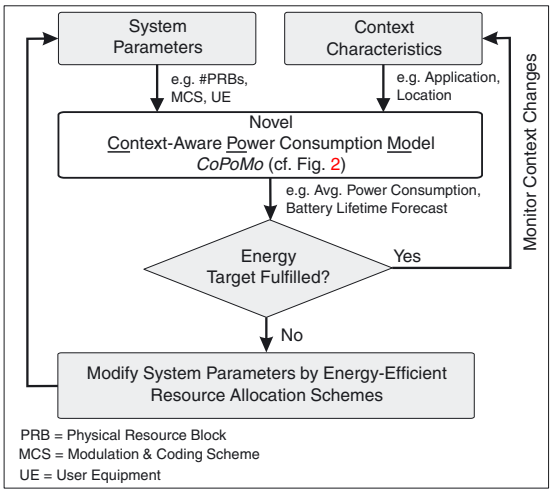

Figure 1. CoPoMo-enabled control loops for energy-efficiency optimization.

Table I. Overview of current power consumption models.

	System parameter			Context parameter		
Model	Tx-power	Allocated PRBs	Device type	Radio channel	Traffic model	LTE specific
Dufkova [11]	D	-	Y	-	D	Y
Somavat [12]	-	-	Y	-	-	-
Saleh [13]	D	-	-	-	-	Y
Lauridsen [14]	D	D	Y	-	-	Y
Jensen [15]	D	-	-	-	-	Y
Dusza [16]	D	D	Y	D	D	D
Fowler [17]	-	-	-	-	S	Y
CoPoMo	**S**	**S**	Y	**S**	**S**	Y

D, Deterministic; S, Stochastic; Y, Yes; -, No.
PRBs, physical resource blocks; LTE, long term evolution; CoPoMo, context-aware power consumption model.

- A reliable battery lifetime forecast taking into account stochastic context parameters (e.g. traffic and channel) as well as system parameters (e.g. allocated physical resource blocks (PRBs), modulation and coding scheme (MCS)),
- a Markovian-based power consumption model to incorporate different traffic characteristics (in the context of real-time and non-real-time applications) and
- the consideration of empirically derived power consumption models for actual, commercially available user equipments (UEs).

Although in this paper we focus on most recent LTE devices, the modelling approach is also applicable to other network technologies, such as LTE Advanced.

The rest of the paper is structured as follows: after discussing the related work (Section 2) and the problem statement (Section 3), we introduce an overview of the components of CoPoMo (Section 4). Then, the LTE device energy model (Section 5), the stochastic Markovian state model (Section 6) and its close to reality parameterisation (Section 7) are presented. To validate CoPoMo, we introduce in Section 8 an independent system simulation, in which the analytical Markovian model has been replaced by a stochastic movement of UE through a realistic cell environment. In Section 9, we present a detailed case study, in which the results of CoPoMo are validated by the simulation.

2. RELATED WORK

Table I provides an overview of selected research results in which various power consumption models have been presented. In [11] and [12], constant power consumption values for a Universal Mobile Telecommunication System (UMTS) UE for idle and active connections are assumed, without the consideration of dynamic system and context parameters. In [13], the traffic parameter throughput is correlated with the emitted power by introducing the throughput power consumption. But Saleh *et al.*[13] do not quantify the relationship between emitted and consumed power, which would be necessary for battery lifetime forecasts. In [14], the optimal relationship between the number of allocated resources, and the average power consumption of an LTE UE is determined by applying a system simulation. The model assumes a traffic pattern with a fixed file size. The duration of the transfer is calculated dependent on the throughput (determined by the number of allocated PRBs and the signal-to-noise ratio (SNR)), leading to variable power consumption values. For the determination of the SNR, an urban single cell scenario is simulated. As LTE devices were not available, a UMTS power consumption model was adopted in combination with LTE system parameters. The first actual measurement of the impact of the uplink transmission power and other system parameters on the power consumption of an LTE UE has been presented in [15]. However, there is no detailed information given on the type of the UE and in how far the results are universally valid for other UE.

Our own previous work presented in [16] firstly introduces a closed-form power consumption model that incorporates empirically derived device parameters together with the uplink transmission power. The presented example application of the model is the suitable dimensioning of batteries for deterministic communication scenarios.

In [17], the power consumption of a device in an idle mode is investigated by means of a Markovian model. The model is leveraged for a performance evaluation of the discontinuous reception (DRX) algorithm in LTE. The stochastic analysis of the scheme allows for realistic forecasting of the possible energy savings dependent on the DRX parameterisation. The achievable gain is provided in terms of ratios without providing quantitative power consumption values.

The overview highlights the need for a holistic, stochastic modelling approach. The analytical CoPoMo model

addresses the full set of parameters introduced in Table I and incorporates stochastic models for the radio channel and the traffic characteristics as a particular novelty of our work. Thereby, quantitative optimizations of the battery lifetime under dynamically changing environments and usage profiles may be enabled.

3. PROBLEM STATEMENT

The overall aim of the proposed model is to quantify the impact of a given system parameter set **S** on the expected value of the battery lifetime T_{Batt} for a given set of context parameters **C** (cf. Figure 1). Assuming a battery energy E_{Batt}, the expected value of T_{Batt} is given by

$$\mathbb{E}\left[T_{\text{Batt}}\right] = \frac{E_{\text{Batt}}}{P_{\Sigma}} \tag{1}$$

with P_{Σ} being the expected value of the power consumption where

$$P_{\Sigma} = \mathbb{E}\left[\bar{P}\right] = \int_{0}^{\infty} \bar{P}(\mathbf{S}) \cdot f_{\bar{P}}(\mathbf{S}, \mathbf{C})\, \mathrm{d}\bar{P}. \tag{2}$$

It is worth noting that the probability distribution $f_{\bar{P}}(\mathbf{S}, \mathbf{C})$ of the instantaneous power consumption $\bar{P}(\mathbf{S})$ depends not only on the system parameterisation but also on the context parameter set **C** that consists of, for example the application characteristic and the cell environment. The system parameter set **S** is given as

$$\mathbf{S} = \{\delta, P_0, M, \alpha, \beta, \gamma, f_c\} \tag{3}$$

with the activity ratio δ, the required uplink transmission power per PRB P_0, the number of allocated PRB M, the device specific parameters α, β and γ as well as the carrier frequency f_c. The context parameter set is given by

$$\mathbf{C} = \{\lambda, D, \kappa, \rho\} \tag{4}$$

with the connection arrival rate λ, the average file size D, the cell environment κ that is characterised by a three-dimensional map incorporating material properties (e.g. of buildings and road) and base station locations as well as the user mobility trajectories ρ.

4. CoPoMo APPROACH AND METHODOLOGY

An overview of different components of CoPoMo is provided in Figure 2. The inputs of the model are the system and context parameter sets **S** and **C** that have been introduced in the previous section.

The parameters feed into several dedicated submodels with different purposes. The empirical power consumption model allows the derivation of power consumption values $\bar{P}_i$ for different power states in which a UE operates (idle, low, high and max). The details of this model and its parameterisation for various, most recent LTE devices are described in Section 5. In order to derive the average power consumption P_{Σ}, we combine the $\bar{P}_i$ values in a dedicated Markovian model (introduced in detail in Section 6) with corresponding state probabilities p_i, which are determined from context-dependent state-transition probabilities in terms of arrival and service rates λ_i and μ_i (cf. Section 7.1). In order to use close to reality values, these probabilities are determined by taking the changing physical channel characteristics into account. Whereas the service rate depends on the physical channel-dependent throughput R (derived from measurements described in Section 7.2), the arrival rate leading to a transition into a dedicated power state depends on the service usage pattern λ as well as the cell environment dependent parameter ϑ_i (cf. Section 7.3 for details). This short overview underlines a key characteristic of the proposed approach: a stochastic Markovian model is combined with the measurement-based parameterisation to produce accurate power consumption results for system developers and operators to design energy-optimised operation and resource allocation schemes.

5. AN EMPIRICAL POWER CONSUMPTION MODEL FOR LTE UE

The determination of the relationship between the emitted transmission power P_{Tx} (dBm) and the power consumption of an LTE-enabled UE $\bar{P}$ (W) is crucial for any reliable power consumption model. Therefore, extensive measurements for different commercially available LTE UE (data sticks and smartphones) have been performed based on a Rohde & Schwarz, Munich, Germany, which allows for full control of the uplink transmission power P_{Tx} independent of the radio channel. For measuring the power consumption of the UE under different system parameterisations, the device is not directly connected to the battery but via an interconnected measurement probe (Hitex Development Tools, Karlsruhe, Germany Power Scale), which samples the consumed power in terms of voltage and current at a frequency of up to 100 K samples/s (see measurement setup in Figure 3 and the photo in Figure 4).

The results of the measurement for a (High Tech Computer Corporation (HTC), Taoyuan, Taiwan) velocity smartphone as well as for a Samsung Galaxy S3 (Samsung Group, Seoul, South-Korea) phone are shown in Figure 5 for both supported frequency bands. One can see from the plot that the power consumption curve can be divided into two pieces: for a low transmission power, below a device specific threshold γ, the graph is characterised by a small slope. For higher values of P_{Tx} the slope is significantly steeper. This specific characteristic can be observed for all investigated UE (cf. Table II). This piecewise characteristic reflects the different stages of the power amplifiers that are used in the state-of-the-art mobile equipment [18]. Furthermore, one can observe the impact of the LTE frequency band on the power consumption. For the application of the

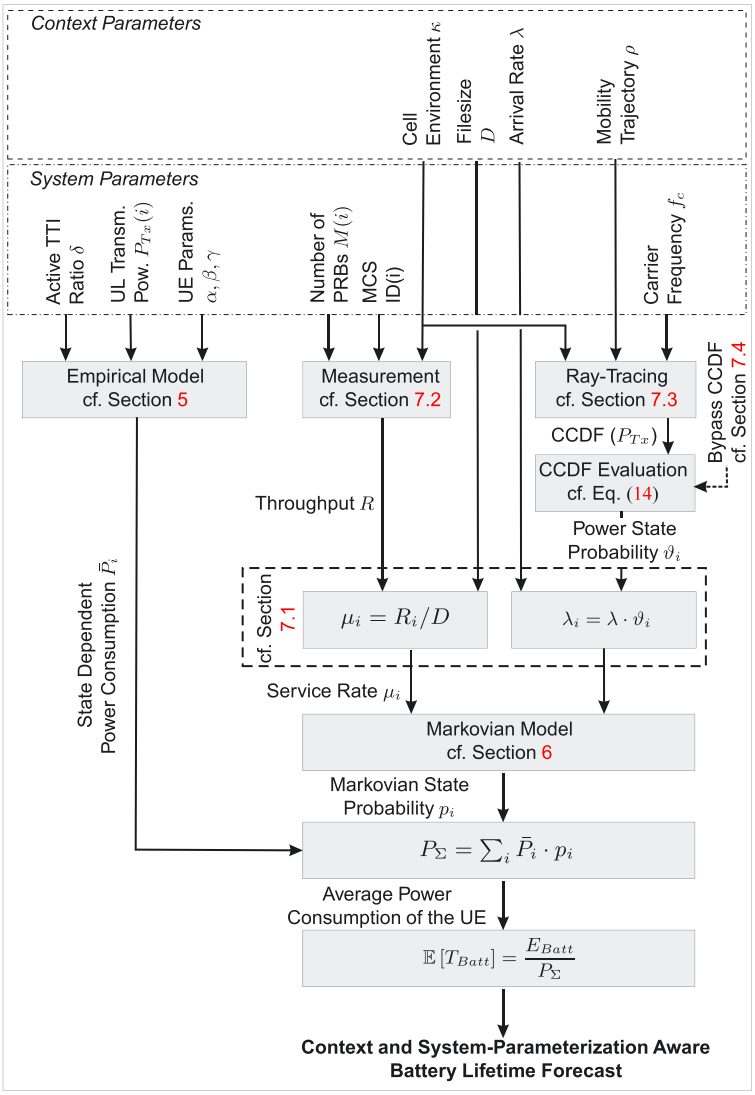

Figure 2. Model parameters and dependencies for stochastic CoPoMo based power modelling (non-real-time case). TTI, Transmit Time Interval; UL, uplink; UE, user equipment; PRBs, physical resource blocks; MCS, modulation and coding scheme; CCDF, complementary cumulative distribution function.

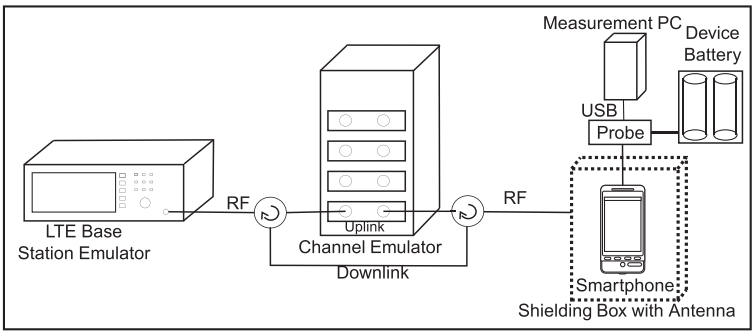

Figure 3. Measurement setup for detailed power consumption measurements. LTE, long term evolution; RF, radio frequency; USB, universal serial bus.

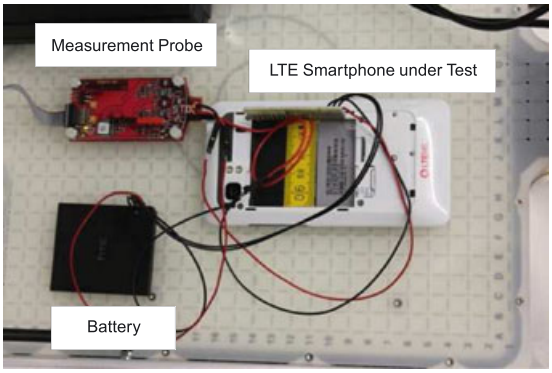

Figure 4. Photograph of power consumption measurement for smartphone. LTE, long term evolution.

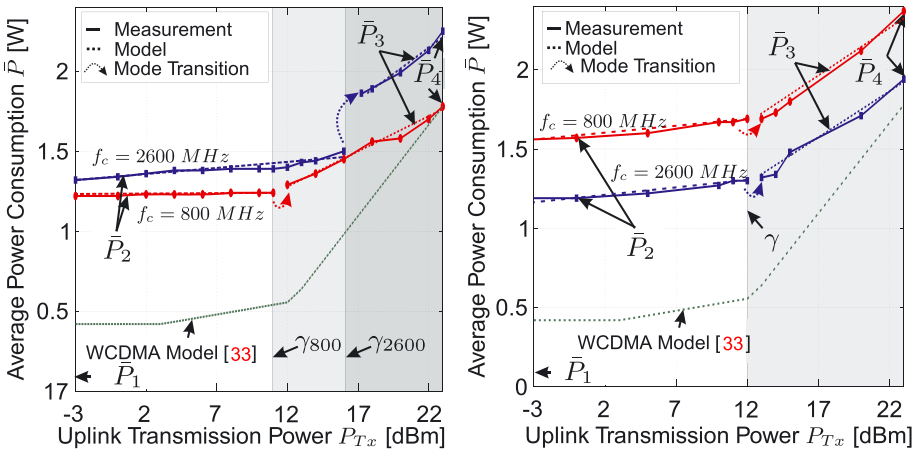

(a) Samsung Galaxy S3. (b) HTC Velocity 4G.

Figure 5. Tx-Power dependent average power consumption versus empirical model for two different smartphones (cf. Table II). WCDMA, wideband code division multiple access.

empirically derived power consumption $\bar{P}$ to CoPoMo, the two curve pieces are independently approximated by linear functions [16]:

$$\bar{P}(P_{Tx}) = \begin{cases} \alpha_L \cdot P_{Tx} + \beta_L & \text{for } P_{Tx} \leq \gamma \\ \alpha_H \cdot P_{Tx} + \beta_H & \text{for } P_{Tx} > \gamma \end{cases} \quad (5)$$

with the device specific parameters α, β and γ as given in Table II and the uplink transmission power P_{Tx}. We derive the value of P_{Tx} from the system parameters with the following considerations: neglecting the closed-loop components of the Transmit Power Control (TPC) formula given in [19] and applying full path loss compensation, P_{Tx} is given by

$$P_{Tx} = \min\left(P_{\max}, P_0 + 10\log_{10}(M) + PL\right) \quad (6)$$

with the maximum transmission power allowed for LTE $P_{\max}$ (23 dBm for class 3 UE [20]), the transmission power per PRB P_0, the number of allocated PRB M and the path loss PL. It is worth noting that the number of allocated PRB has a direct impact on P_{Tx} and therefore, the power consumption. The empirically derived values given in Table II should be interpreted as follows: the parameter β_L determines the power consumption for $P_{Tx} = 0$ dBm, which is a typical value for the low power state. For a given value of P_{Tx}, the Samsung Galaxy S3 smartphone, for example, consumes more power if it is operating at 2600 MHz ($\beta_L = 1.3$ W) than in the 800 MHz case ($\beta_L = 1.2$ W). For higher values of P_{Tx}, the power consumption of the smartphone increases along a slope that is defined by α_H. Whereas for the 800 MHz case, the value of α_H is relatively small ($\alpha_H = 43$ mW/dBm), the power consumption is increasing much faster for the case of 2600 MHz ($\alpha_H = 89$ mW/dBm). The maximum error given in Table II gives the maximum deviation of the model given in Equation (5) from the actual measurements.

The measurements do furthermore show that the reception of data does not cause a significant additional energy consumption if the UE is actively transmitting data in

Table II. Empirical model parameters for different long-term evolution user equipments (extended version of table presented in [16]).

Model parameter	HTC Velocity 4G (Smartphone)		Samsung Galaxy S3 (Smartphone)		Samsung GT-B 3740	Samsung GT-B 3730	Huawei E 398		Sierra Wireless AC 330U	
Frequency (MHz)	800	2600	800	2600	800	2600	1800	2600	2100	2600
α_L (mW/dBm)	4.8	4	1.6	7.2	7.7	7.2	10	12	5.6	5.4
β_L (W)	1.6	1.2	1.2	1.3	1.6	1.6	1.7	2	1.6	1.9
α_H (mW/dBm)	68	61	43	89	130	54	24	68	27	28
β_H (W)	0.79	0.52	0.77	0.2	0.4	1.5	1.9	1.4	1.5	1.8
γ (dBm)	12	12	11	16	11	10	16	16	16	16
Maximum error (per cent)	4.1	3.5	3.2	3.5	1.7	3.9	4.7	1.6	3.6	1.5
$\bar{P}_1$ (mW)	40	40	36	36	175	44	236	236	63	63
$\bar{P}_2$ (W)	1.6	1.2	1.2	1.3	1.6	1.6	1.7	2	1.6	1.9
$\bar{P}_3$ (W)	1.98	1.59	1.5	1.94	2.61	2.39	2.37	2.73	2.03	2.35
$\bar{P}_4$ (W)	2.35	1.92	1.76	2.25	3.3	2.74	2.45	2.96	2.12	2.44

parallel (full duplex). Nevertheless, for pure data reception, the UE must leave the idle state towards the Radio Resource Control connected state. The power consumption in this state is however independent of any external parameter (cf. [15]) and can be modeled by β_L.

6. A STOCHASTIC MODEL OF LTE UE POWER CONSUMPTION BASED ON MARKOV CHAINS

We assume that an LTE UE will enter different power states while randomly moving through an LTE network depending upon the spatiotemporal variations of the radio channel. To describe this stochastic process, we introduce a Markov chain with a state space of four different power states (cf. Figure 6):

(1) *Idle*: In this state, the UE is not transmitting any data. The radio frequency components are disabled (despite regular observation of the broadcast channel) and the energy consumption is reduced to a device dependent minimum $\bar{P}_1$. The power consumption does not depend upon any external system or context parameters.
(2) *Low*: In the low power state of the UE for data transmission, the TPC algorithm of LTE adjusts the transmission power in a way that a predefined target SNR SNR_T at the base station can be achieved. The power consumption is chosen to be $\bar{P}_2 = \bar{P}(P_{Tx} =$ 0 dBm) (cf. Equation (5)).
(3) *High*: If the overall transmission power P_{Tx} obtains higher than a device specific threshold γ, the high power state of the UE is entered. The power consumption is chosen to be $\bar{P}_3 = \bar{P}(P_{Tx} = (P_{\max} + \gamma)/2)$. This simplification will be validated by simulation in Section 9.
(4) *Max*: If the TPC algorithm can no longer achieve the target SNR by compensating for the path loss, the maximum power state is entered. In this state, the UE is transmitting at the maximum allowed transmission power $P_{\max}$, which comes along with a high average power consumption $\bar{P}_4 = \bar{P}(P_{Tx} = P_{\max})$.

The device specific values of P_1, P_2, P_3 and P_4 used for the model are given in Table II. Knowing the state probabilities p_i together with the average deterministic state power $\bar{P}_i$, one can calculate the long-term average power P_Σ as

$$P_\Sigma = \sum_i \bar{P}_i \cdot p_i \tag{7}$$

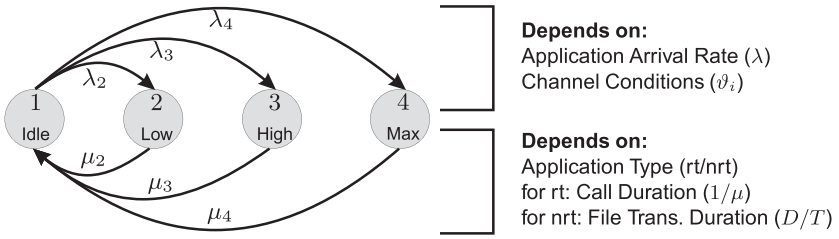

Figure 6. A Markovian model for power consumption of long-term evolution user equipment.

from that the approximated average battery lifetime T_{Batt} is

$$T_{\text{Batt}} = \frac{E_{\text{Batt}}}{P_{\Sigma}} \tag{8}$$

with the available battery energy E_{Batt} (Wh). For this purpose we assume that E_{Batt} is independent of the actual power consumption $\bar{P}_i$ [21].

In order to keep the model as simple as possible, we deliberately omitted the direct state transitions between the different active states (cf. Figure 6). This can be carried out without loss of generality because, referring the Little's Law [22], the ultimate parameter that influences the battery lifetime T_{Batt} is the offered traffic λ/μ (cf. Equations (9)–(12)). This allows us to virtually cut one large transmission into a sequence of smaller pieces for which the channel conditions can be assumed to be stationary. Therefore, the simplified Markovian model allows for quite simple mathematical expressions for the state probabilities p_i that are derived by solving the equilibrium condition [23] based on the transition probabilities λ_i and μ_i:

$$p_1 = \frac{1}{1 + \frac{\lambda_2}{\mu_2} + \frac{\lambda_3}{\mu_3} + \frac{\lambda_4}{\mu_4}} \tag{9}$$

$$p_2 = \frac{\frac{\lambda_2}{\mu_2}}{1 + \frac{\lambda_2}{\mu_2} + \frac{\lambda_3}{\mu_3} + \frac{\lambda_4}{\mu_4}} \tag{10}$$

$$p_3 = \frac{\frac{\lambda_3}{\mu_3}}{1 + \frac{\lambda_2}{\mu_2} + \frac{\lambda_3}{\mu_3} + \frac{\lambda_4}{\mu_4}} \tag{11}$$

$$p_4 = \frac{\frac{\lambda_4}{\mu_4}}{1 + \frac{\lambda_2}{\mu_2} + \frac{\lambda_3}{\mu_3} + \frac{\lambda_4}{\mu_4}} \tag{12}$$

One concrete application example of the Markovian model is presented in Figure 7 where the stacked bars show a context-dependent distribution of state probabilities p_i together with the corresponding average power consumption P_{Σ}. How the context parameters can actually be incorporated by the state-transition probabilities, and therefore, the state probabilities will be described in detail in the following section.

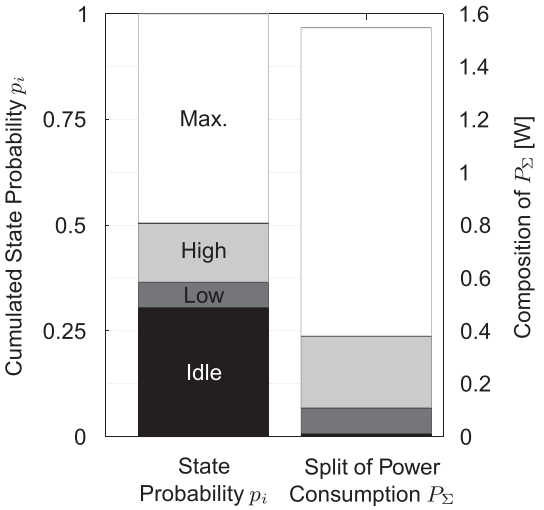

Figure 7. Examples of state probability distribution and corresponding power consumption split (HTC Velocity 4G).

7. CONTEXT-DEPENDENT PARAMETERISATION BY MEASUREMENTS AND RAY-TRACING

Without loss of generality, the previously described generic model is parameterized based on measurements and specialised simulations. For the determination of every single parameter, extensive investigations based on commercially available hardware, close to reality mobile radio channels and sophisticated ray-tracing simulations have been performed. In this section, the parameterisation methods as well as the results and the implications for the model are described in detail.

7.1. Determining context-dependent state-transition probabilities

In this subsection, we determine – for non-real-time and real-time applications – first the transition probabilities λ_i for a UE entering a specific power state and then the state-transition probabilities μ_i for leaving the state (cf. Table III).

Table III. Application-context-dependent state-transition probabilities.

Model parameter	Real time application	Non-real-time application
$1/\lambda$	Avg. inter-arrival time of, for example, voice calls	Avg. inter-arrival time of files
$1/\mu$	Avg. call duration	Avg. transmission duration (state dependent)
λ_i	$\lambda \cap \vartheta_i$	$\lambda \cap \vartheta_i$
μ_i	μ	R_i/D

Avg., average.

The overall probability that a transmission (data or voice call) starts, and therefore, the model is leaving the idle state towards any of the other states follows a negative exponential distribution with a mean value λ [24]. The scenario-dependent probability that the UE has to be operated in a specific power consumption state (low, high or max) is given by ϑ_i. The state-transition probabilities λ_i follow the compound probability of λ and ϑ_i and are given by

$$\lambda_i = \lambda \cap \vartheta_i = \lambda \cdot \vartheta_i \quad \text{with} \quad \sum_i \vartheta_i = 1, \quad i = 2...4. \tag{13}$$

A challenge in this context is the suitable choice of ϑ_i considering the specific radio channel conditions as well as cell specific parameters such as the target SNR (cf. Section 7.3).

For the determination of suitable values of μ_i, one has to be aware of the different Quality of Service requirements of different kinds of applications. For rt applications such as Voice over Internet Protocol (VoIP), the service rate is negative exponentially distributed with a mean value μ [24] but independent of any other parameters. Therefore, $\mu_i = \mu$. On the other hand, for data transfer applications, the service rate is calculated by dividing the available throughput R_i, which depends on the SNR-dependent MCS used as well as the number of allocated PRBs (cf. Figure 2) by the file size, which is negative exponentially distributed with a mean value D. If the channel quality in terms of the SNR decreases (e.g. in the maximum power state), less PRBs are assigned, which leads to a longer file transfer duration and therefore, a decreased value of μ_i. Table III summarises the interdependencies for real-time and non-real-time applications.

7.2. Radio channel-aware throughput measurements

In the previous section, we have shown that the achievable throughput in the different states R_i has a major impact on the service rate μ_i for non-real-time applications. For the quantification of the impact of the mobile radio channels on the throughput, laboratory measurements using a radio channel emulator were performed (cf. Figure 3). In [25], we presented detailed results based on this setup. For the low power state or high power state, the throughput R_2 or R_3 is determined by the target SNR, whereas for the maximum power state, the throughput R_4 is reduced because the path loss cannot be completely compensated by the TPC algorithms due to the maximum transmission power restriction [26].

7.3. Ray-tracing simulations of close to reality SNR distributions

The probability ϑ_i that a UE at a randomly chosen position inside the cell will enter state i for data transmission is significantly influenced by the environment. This includes the cell radius as well as the frequency band, building density, antenna patterns and many more cell specific parameters. Figure 8 illustrates the spatial distribution of the three active states of the UE (low, high and max) for one example environment. An UE moving through the cell cuts across different areas, whereas the probability ϑ_i corresponds to the relative ratio of the three different zones in Figure 8.

To determine the position-dependent transmission power $P_{Tx}(x, y)$, we use ray-tracing simulations for a fixed SNR_T. In Figure 9, the complementary cumulative distribution function (CCDF) of the location-dependent

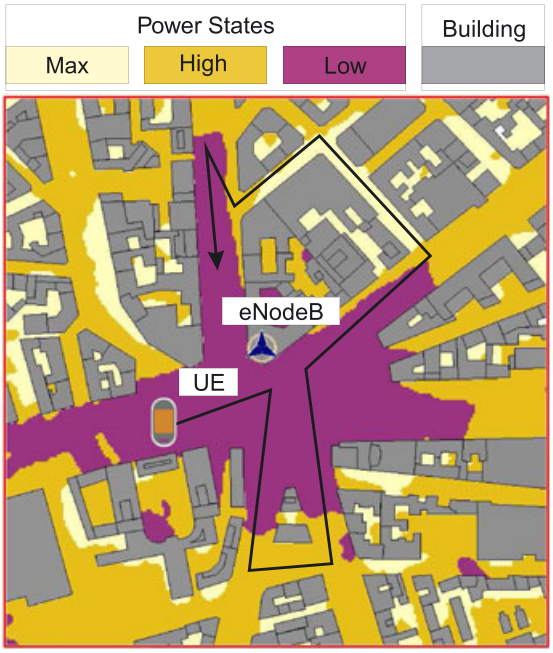

Figure 8. An illustration of the spatial power mode distribution in an example environment. UE, user equipment.

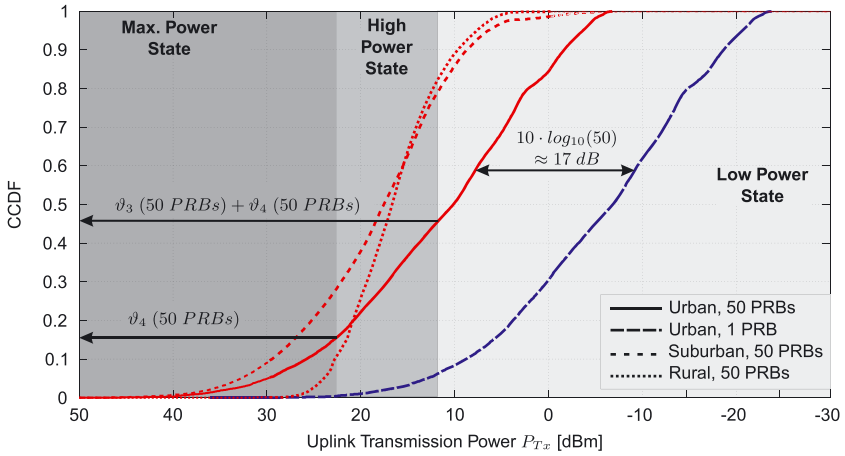

Figure 9. Complementary cumulative distribution function of the transmission power for various cell environments and different physical resource block (PRB) allocations.

uplink transmission power is shown for different example scenarios. One can see that the slope does strongly depend on the scenario. The steeper the slope is the higher becomes the probability that the transmission state changes even for minor variations of the radio channel conditions. From the CCDF, one can derive the probabilities ϑ_i that a transmitting UE has to enter state i for achieving SNR_T:

$$\begin{aligned}\vartheta_2 &= 1 - P[P_{Tx} > \gamma] \\ \vartheta_3 &= P[P_{Tx} \geqslant \gamma] - P[P_{Tx} \geqslant P_{\max}] \\ \vartheta_4 &= P[P_{Tx} > P_{\max}]\end{aligned} \tag{14}$$

It is worth noting that the ϑ_i depend on the number of actually allocated PRBs M.

The CCDF derived from the ray-tracing simulation is furthermore used to determine the impact of the maximum power state on the achievable throughput T_4 (non-real-time) as well as the needed number of PRBs (real time). For such purpose, the virtual transmission power P_v (dBm) that would be needed for achieving SNR_T (dB) in the maximum power state is taken from the CCDF as a weighted average. As P_v cannot be used because of the power limitation of the UE, in the maximum power state, the actual SNR is no longer the target SNR but decreased to $SNR_{\max} = SNR_T - (P_v - P_{\max})$. For non-real-time services, this effect is usually compensated by assigning a lower number of PRBs $M_{\max}$ [14, 26]. For CoPoMo, this behaviour is achieved by calculating $M_{\max}$ as

$$M_{\max} = \left\lfloor M \cdot \left(10^{\left(\frac{SNR_T - SNR_{\max}}{10} \right)} \right)^{-1} \right\rfloor \tag{15}$$

For real-time applications the actual value of $SNR_{\max}$ is directly used for the determination of the needed MCS and the corresponding number of PRBs needed for maintaining the required data rate.

7.4. Consideration of uplink interferences

In the previous section, it has been shown how ray-tracing simulations can be used to incorporate the impact of the cell environment on the battery lifetime. Nevertheless, this particular method is not capable to reliably model the impact of inter-cell interferences in the uplink. The reason for this is that the extent of this particular impairment does strongly depend on the applied interference avoidance schemes [27] as well as on the user distribution. In case that uplink inter-cell interferences cannot be neglected (e.g. because the same frequencies are used in neighbouring cells), they affect the distribution of the transmission power that is required for maintaining the desired SNR_T. More precisely, a larger amount of interferences leads to an increased probability for a higher transmission power as well as to a decreased throughput for those users that are operating their UE in the maximum power state (cf. Equation (15)). As CoPoMo reflects the impact of interferences on the UE power consumption entirely by the respective CCDF of the transmission power, only this distribution needs to be adapted. As one can see from Figure 2, the ray tracing can be bypassed for this purpose, that is, a CCDF of the transmission power can directly be fed to the model. Suitable methods on how to derive interference-aware transmission power distributions, incorporating the user distribution as well as the applied interference avoidance schemes, are presented in [28] (simulation) and [29] (analytic model).

8. SYSTEM SIMULATION FOR VALIDATION

The results of the Markovian model are validated by an independent system simulation. In Figure 10, the model parameters and dependencies for simulation based power

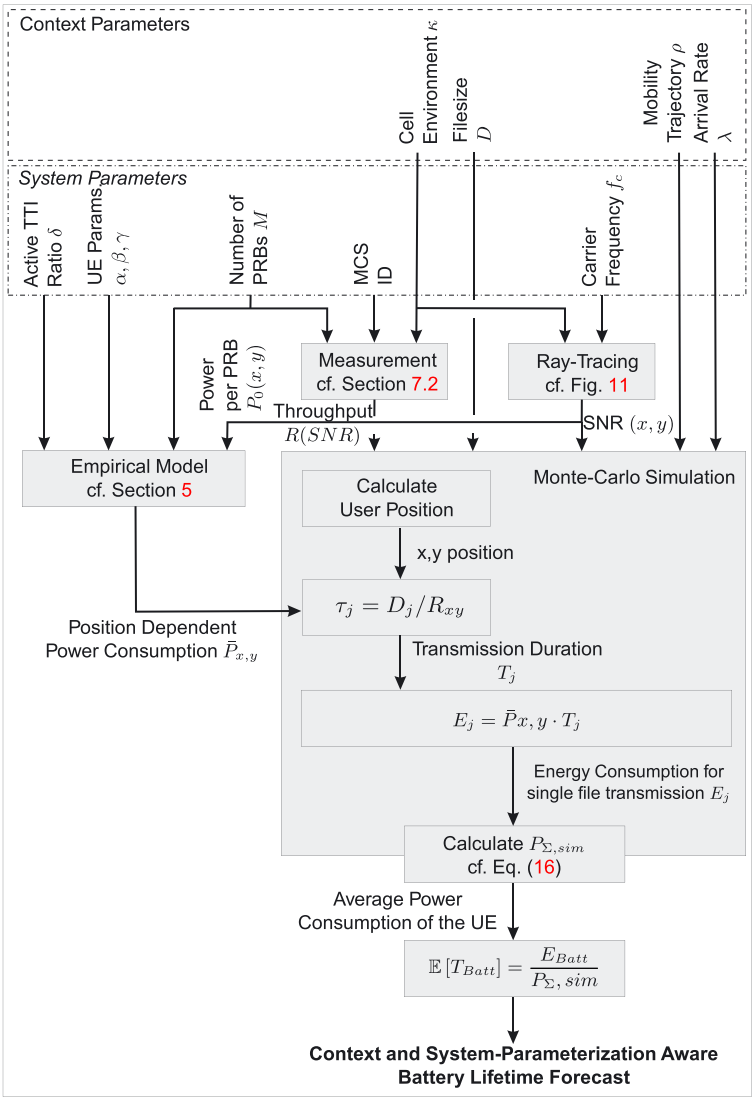

Figure 10. Parameters and dependencies for system simulation based model validation (non-real-time case). TTI, Transmit Time Interval; UL, uplink; UE, user equipment; PRBs, physical resource blocks; MCS, modulation and coding scheme; SNR, signal-to-noise ratio.

consumption modelling can be found. Here, the same context and system parameters are used as in Figure 2. It can be seen that we replaced the stochastic component of the model to validate the determination of the average power consumption.

For this purpose, we use the same ray-tracing scenarios (urban, suburban and rural) that are used for the stochastic model, but instead of characterising the channel conditions by a CCDF, a user is moving through the environment following an user defined mobility model.

For the user mobility, the scenarios are divided into square cells with the same grid size as that in the ray-tracing simulation. For each step of the mobility, it is checked whether the neighbour-grid cells are open areas. The simulated user then moves to one of the free neighbour-grid cells according to the mobility model. After a walking duration T_{IDLE} a transmission begins. The connection duration T_j for transmission j and the transmission power P_{Tx} (from ray-tracing results) are determined individually for calculating the energy of a single transmission $E_j = \bar{P}_{x,y} \cdot T_j$. Thereby, $\bar{P}_{x,y}$ is gained from the continuous power consumption model (cf. Equation (5)) with device parameters from Table II. At the end of the simulation, the average consumed power $P_{\Sigma,\mathrm{sim}}$ can be calculated through dividing the total energy, including the mean value of all single data transmissions' energy consumption and idle time energy consumption, by the total simulation duration:

$$P_{\Sigma,\mathrm{sim}} = \frac{\sum_{j=1}^{A\cdot B} \left(E_j + P_{\mathrm{IDLE}} \cdot T_{\mathrm{IDLE},j}\right)}{\sum_{j=1}^{A\cdot B} \left(T_j + T_{\mathrm{IDLE},j}\right)} \tag{16}$$

The primary goal of the simulation is to validate the assumption needed for the analytical CoPoMo. The three most important differences between the two solution approaches are that the analytical model

- discretises the power consumption model to only three active states (cf. Figure 5),
- assumes a perfectly uniform user distribution represented by only statistic parameters and
- uses only one constant value of $M_{\max}$ (cf. Equation (15)) for the number of actually assigned PRB in the maximum power state.

The following case study illustrates that in spite of these differences, the power consumption estimation by CoPoMo matches with the simulation result very well.

9. CASE STUDY: SCALABLE POWER CONSUMPTION BY CONTEXT-AWARE RESOURCE ALLOCATION

In this section, an example application of CoPoMo is described, which focuses on context-dependent resource allocation for battery lifetime extension as well as a suitable system parameter optimization. Specifically, the impact of the context parameters on the average power consumption is investigated for real-time and non-real-time applications independently.

9.1. Example scenario and parameterisation

For the concrete quantitative results presented in this case study, the device models for a HTC Velocity LTE smartphone and a Samsung Galaxy S III smartphone (cf. Table II) are used. The impact of the cell environment is incorporated by applying ray tracing results for the following:

- three different cell environments (cf. Figure 11) representing urban, suburban and rural scenarios in terms of cell size and building density and
- two different carrier frequencies (LTE Band 7 @ 2600 MHz and LTE Band 20 @ 800 MHz).

The parameterisation of the environments is based on the 3rd Generation Partnership Project (3GPP) reference scenarios given in [31]. The most important ray-tracing parameters are summarised in Table IV.

The throughput that is achievable for different radio channel conditions has been measured in the laboratory based on commercially available UE as described in [25]. For the case studies presented in this paper, we use the so derived SNR dependent throughput for a pure additive white Gaussian noise (AWGN) channel as well as the Extended Pedestrian A multipath fading channel presented in [32].

In all of the plots presented in the following subsections, the results of CoPoMo are shown together with the results derived from corresponding system simulations. The mobility model applied to the system simulation is a multiple start-point random walk approach (cf. Figure 12). This model performs a variety of independent random walks starting in different areas of the overall map. For this

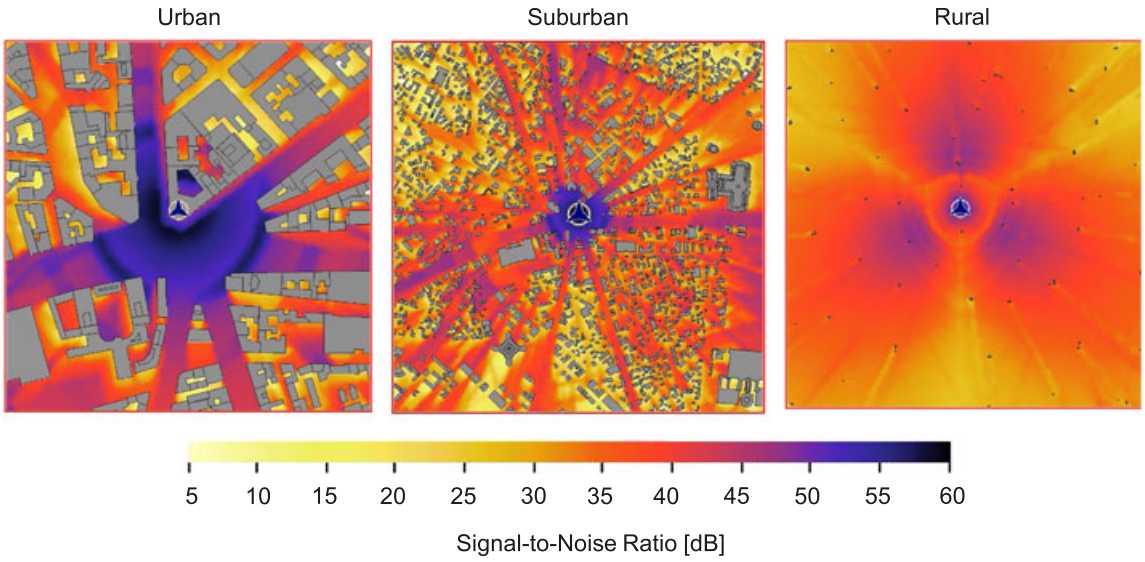

Figure 11. Uplink signal-to-noise ratio distribution for different cell scenarios at 800 MHz carrier frequency and 40 dB transmission power.

Table IV. Ray-tracing parameters and their values.

Ray-tracing parameter	Value
Ray-tracing model	3D intelligent ray-tracing [30]
Propagation class	Double reflection, single diffraction
UE antenna gain	1 dBi
UE noise figure	6 dB
BS antenna opening angle	120°
Antenna downtilt	5°
Inter-site distance urban	500 m [31]
Inter-site distance suburban	1732 m [31]
Inter-site distance rural	5000 m
Noise	Thermal noise

UE, user equipment; BS, base station.

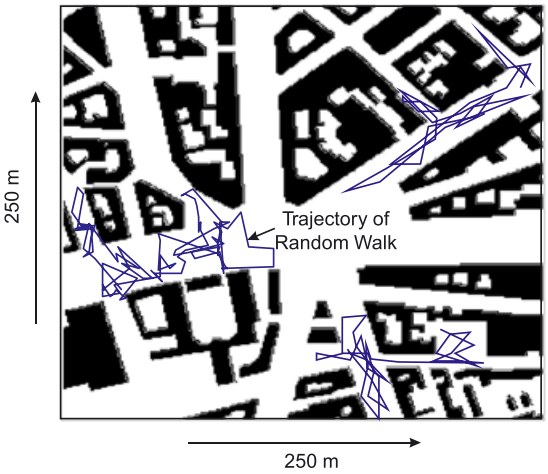

Figure 12. Multiple start-point random walk mobility used for the case studies.

particular mobility pattern, the standard deviation of the simulation has been determined to be below 0.5 per cent for 10^6 simulation steps realised by $A = 1000$ independent random walks incorporating $B = 1000$ transmissions each.

9.2. Power efficient non-real-time applications

9.2.1. Quantifying the context-dependent battery lifetime.

A major advantage of CoPoMo compared with the models presented in literature is the precise quantifiability of the expected context-dependent battery lifetime T_{Batt}. The impact of the cell environment, the carrier frequency and the traffic on the battery lifetime has been reflected by the variable state probabilities p_i (cf. Section 6). Figure 13 shows how the context influences the probabilities that the UE operates in the idle, low, high or maximum power state for two different scenarios (derived by CoPoMo estimations and system simulation independently). Although for low traffic (e.g. $\lambda = 1/1000$ min), the idle state dominates in both scenarios; there is a significantly differing characteristic observable for higher values of λ (e.g. $\lambda = 10/\text{min}$). Although, for example, in the urban/pedestrian/800 MHz scenario, the maximum power state is the most probable one; this phenomenon changes towards the high power state for a rural/AWGN/800 MHz scenario. These context-dependent values of p_i directly influence the average power consumption P_Σ (cf. Equation (7)) and therefore, T_{Batt}.

This impact can be observed in Figure 14 where P_Σ as well as the approximated battery lifetime for an HTC Velocity 4G smartphone are shown for different application arrival rates. For this purpose, the available energy E_{Batt} of the smartphone battery is assumed to be $E_{\text{Batt}} = 6$ Wh. The system parameterisation (50 continuously allocated PRB) is chosen for a worst case scenario from a power consumption perspective. One can see that for low traffic (cf. Figure 14 (1)), the average power consumption P_Σ converges towards $\bar{P}_{\text{IDLE}}$ for $\lambda \to 0$. This is because the UE is in the idle state for most of the time (cf. Figure 13). For very high values of λ (cf. Figure 14 (2)), the UE is almost continuously active, and P_Σ converges towards a maximum, which contingents on the context-dependent values of p_i as well as the device parameters for the specific LTE frequency band. For an average application arrival rate of $\lambda = 1/10$ min (cf. Figure 14 (3)), which could correspond to Web-surfing usages, for example, via multimedia applications such as Instagram[‡], one can observe a significant impact of the context. Whereas in an rural/AWGN/800 MHz scenario, a battery lifetime of about 60 h can be achieved, the battery needs to be recharged after 9 h if the scenario is suburban/pedestrian/800 MHz and after only 7 h in an urban/pedestrian/2600 MHz scenario. However, for extremely high traffic and therefore, a continuous data transmission, the 2.6 GHz system is more power efficient than the 800 MHz system. This effect is due to the higher efficiency of the considered HTC Velocity 4G smartphone at this frequency band (cf. Figure 5). In addition to this, Figure 14 shows the output of the model presented in [14] ($PL = 100$ dB, Noise $\widehat{=} -128$ dBm). Although the results by the wideband code division multiple access model [14] are suitable for relatively low traffic, significant differences can be observed for the wide range of D shown in Figure 14. These are due to different device models (cf. Figure 5), and the fact that CoPoMo also encapsulates scenario specific context parameters. Furthermore, Figure 14 illustrates the impact of interferences on the battery lifetime. For this purpose, the CCDF bypass described in Section 7.4 has been applied with the interference-enabled CCDF of the transmission power from [28] (assuming fair allocation and slow power control (FA-SPC)). From the results can quantify the significant

[‡]www.Instagram.com

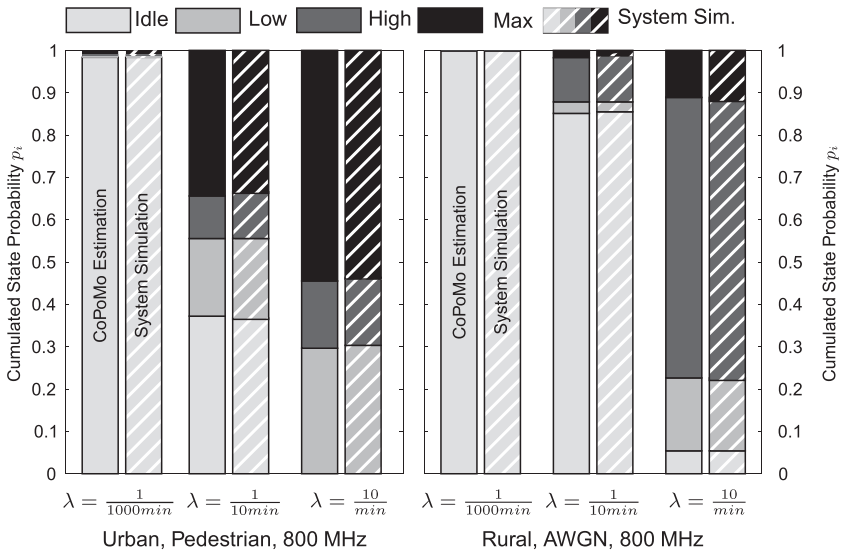

Figure 13. State probability (respectively relative frequency for system simulation) p_i for different traffic characteristics and cell environments (SNR_T =13 dB, D = 10^8 Bit, $M = 50$).

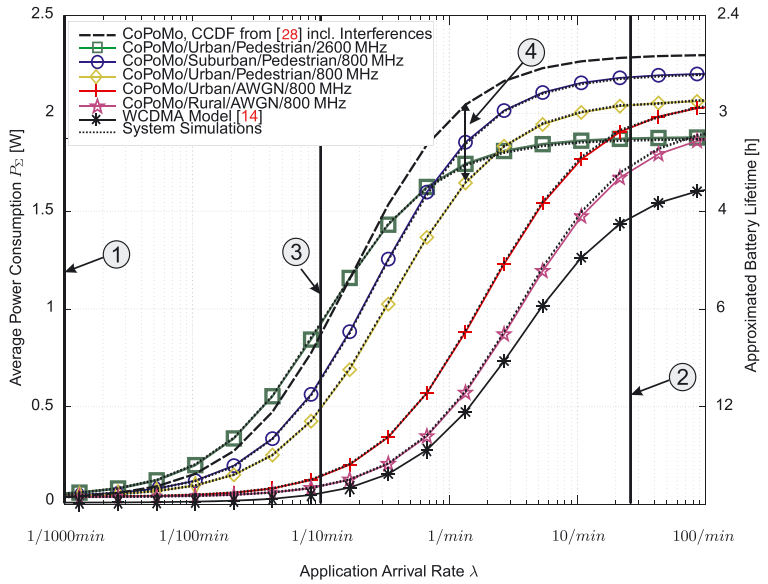

Figure 14. Impact of the cell environment on the average power consumption for different traffic characteristics including validation by system simulation (HTC Velocity 4G, D = 10^8 Bit, $M = 50$ (continuously allocated), SNR_T =13 dB, $E_{\text{Batt}} = 6$ Wh), comparison with wideband code division multiple access (WCDMA) model **[14]** and impact of interferences (assuming device parameters for 800 MHz and fair allocation and slow power control scheme **[28]**). CoPoMo, context-aware power consumption model; CCDF, complementary cumulative distribution function.

negative impact of interferences on the expected battery lifetime (cf. Figure 14 (4)).

9.2.2. Energy-saving PRB allocation.

With the knowledge of various impact factors on the UE energy efficiency, we can now focus on possible energy-saving approaches. As LTE incorporates orthogonal frequency division multiple access as the multiple access scheme, the available physical resources can be allocated not only in the frequency domain but also in the time domain. The number of simultaneously allocated PRBs in the frequency domain is referred to as M (maximum 50 for 10 MHz LTE system). In the time domain, the smallest assignable resource is one Transmit Time Interval (TTI) of

1 ms [19] consisting of two consecutive PRB. Therefore, in one radio frame of 10 ms an overall number of 1000 PRBs is available (including control channels). Assuming that for example a certain number of $x = 400$ PRBs is assigned to one user in one frame, there are several possibilities to allocate the resources in the time/frequency grid. In case of a time continuous allocation, the user would obtain $M = 20$ PRBs in each of the 10 TTI. One alternative would be, to allocate $M = 40$ PRBs in the frequency domain but only in 5 out of 10 TTI. Figure 15 illustrates the different possibilities.

The figure illustrates the effect that increasing the number of allocated PRB in the frequency domain M leads to a higher throughput and therefore, a decreasing transmission duration $1/\mu$. If this effect should be compensated, that is, because the overall number of resources assigned to the UE should remain constant regardless the actual resource allocation in the time/frequency grid, the fraction of active TTI has to be reduced with respect to the increase of M.

Assuming that in the idle TTI, an average power of $\bar{P}_1$ is consumed; the overall average power consumption is given by

$$\bar{P} = \frac{1}{L+K} \cdot \left(L \cdot \bar{P}_1 + \sum_{i=1}^{K} \bar{P}\left(P_{Tx,i}\right) \right) \tag{17}$$

with K being the number of active TTI and L being the number of idle TTI. The results presented in Figure 16 quantitatively illustrate the effect of different PRB allocations on the average power consumption. Using as many PRBs as possible in one TTI and then, falling into the sleep mode for a duration as long as possible is intuitively the most energy efficient option. However, CoPoMo allows for a quantitative analysis of the battery lifetime enhancements and suggests resource allocation schemes for achievable energy savings. Figure 16 (1), for example, shows that power savings of up to 73 per cent are possible if four additional PRBs are spent in each active TTI. Nevertheless, this

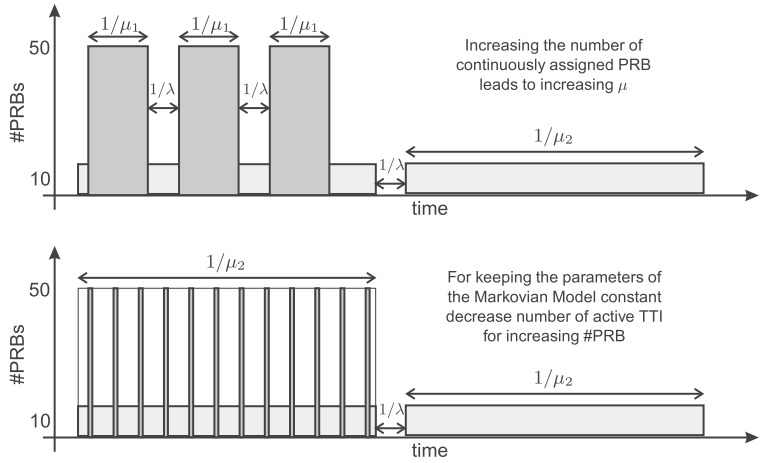

Figure 15. Illustrations of resource allocation schemes and Markovian parameters for fixed (top) and variable (bottom) #PRB/Frame. PRB, physical resource block; TTI, Transmit Time Interval.

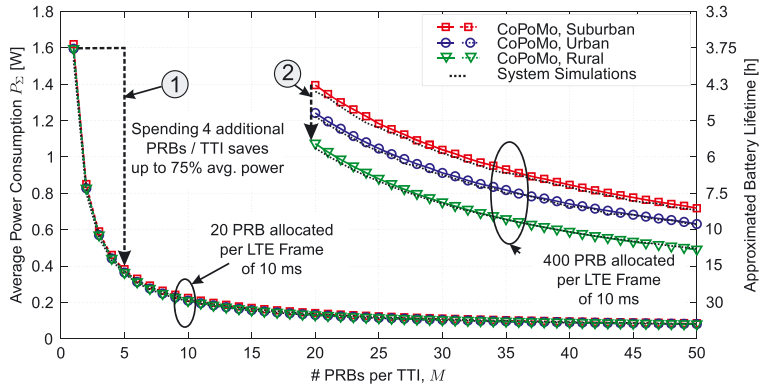

Figure 16. Battery lifetime aware physical resource block (PRB) allocation in time and frequency domain for non-real-time applications (HTC Velocity 4G, urban cell environment, additive white Gaussian noise channel, $f_c = 800$ MHz, $D = 10^9$ Bits, $\lambda = 1/300$ s, SNR_T =13 dB, $E_{\text{Batt}} = 6$ Wh). TTI, Transmit Time Interval; LTE, long term evolution; CoPoMo, context-aware power consumption model.

approach is a suitable solution especially for a small number of PRBs per frame (e.g. 20 PRBs/frame in Figure 16). Beyond that, Figure 16 illustrates the impact of the actual cell environment on the results. One can observe that for relatively low PRB allocations, the cell environment has a negligible impact on the power consumption. This is because for this particular case, the scenario independent idle power is a dominating factor. However, for the case of 400 PRBs per subframe, one can observe a significant impact of the scenario (cf. (2) in Figure 16). More precisely, the power consumption in a suburban environment is the highest, whereas the longest battery lifetime can be achieved in a rural environment. This observation correlates to the CCDF in Figure 9 as the suburban environment is characterised by the highest possibility for the disadvantageous maximum power state.

9.2.3. Impact of the device type on battery lifetime.

Beside the system and context parameters, the hardware specific device parameters α, β and γ (cf. Table II) have a significant impact on the expected battery lifetime as they are directly influencing the state-dependent power consumption values $\bar{P}_i$. For the devices that are supporting multiple frequency bands, it is furthermore important which one of the supported frequency bands is the more power efficient one. Figure 17 illustrates this influencing factor for two smartphones with quite contrary characteristics.

The most important difference is that the HTC Velocity 4G phone is more power efficient at a carrier frequency of 2600 MHz, whereas the Samsung Galaxy S III performs better at 800 MHz (cf. Table II). Combining this fact with the much more advantageous radio channel conditions at 800 MHz leads to the significantly differing battery lifetimes for the device/frequency combinations shown in Figure 17. Whereas the lower path loss at 800 MHz (i.e. a lower average transmission power) is constructively interacting with the already lower power consumption in case of the Galaxy smartphone, a trade-off between the advantageous propagation conditions and the disadvantageous power efficiency at 800 MHz can be observed for the Velocity phone. This trade-off leads to the result that for the particular example scenario shown in Figure 17, the UE is operated more efficiently at 800 MHz for lower traffic, that is $\lambda < 2/\text{min}$, and at 2600 MHz for high traffic, that is, $\lambda > 2/\text{min}$ (cf. (1) in Figure 17). The Samsung phone on the other hand is significantly more efficient at 800 MHz for any system load. The case study therefore illustrates one additional application field of CoPoMo, which is a benchmarking of commercially available smartphones in terms of their battery lifetimes under fair and controllable conditions while incorporating all relevant system and context parameter.

9.2.4. Impact of the carrier frequency on battery lifetime.

Compared with previous cellular systems, LTE is deployed with a quite large set of different carrier frequencies. Assuming that if more than one LTE band is available at a certain location, a switching between the different carrier frequencies is possible. This procedure is called inter-frequency handover. However, the decision which one of the available frequencies is the optimal choice is nontrivial and depends on the actual device type as well as the context. As one can see from Figure 17, performing a handover from 2600 to 800 MHz may allow for significant battery lifetime enhancements of up to 40 per cent (in case of a Samsung Galaxy S III UE, cf. (2) in Figure 17). Nevertheless, the same proceeding may cost up to 10 per cent battery lifetime if another device type is used (i.e. HTC Velocity 4G). Applying this knowledge, a context-dependent optimal system parameterisation can be dynamically chosen by CoPoMo as depicted in Figure 1.

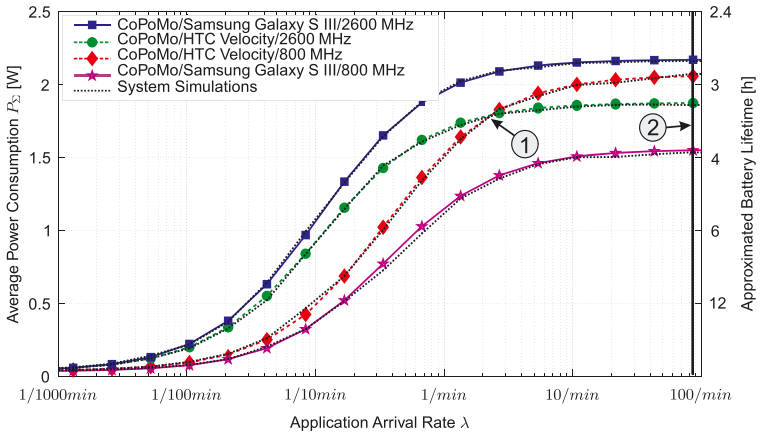

Figure 17. Impact of the user equipment on the average power consumption for different traffic characteristics including validation by system simulation (suburban scenario, pedestrian radio channel, $D = 10^8$ Bit, $M = 50$ (continuously allocated), SNR_T =13 dB, $E_{\text{Batt}} = 6$ Wh). CoPoMo, context-aware power consumption model.

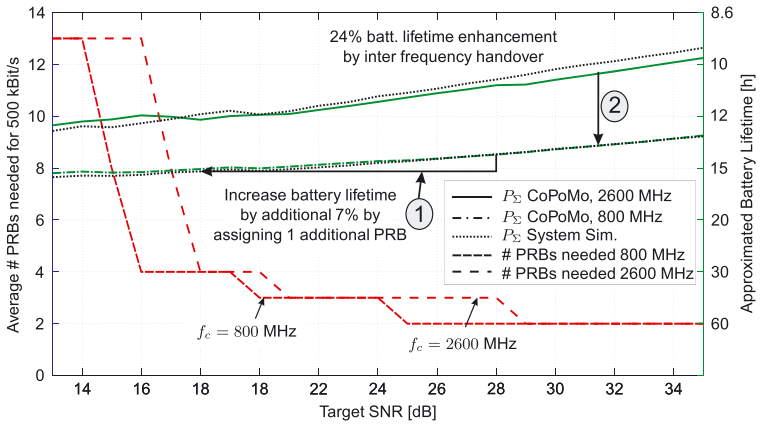

Figure 18. Trade-off between spectrum allocation and power consumption for real-time applications (Samsung Galaxy S III, urban environment, additive white Gaussian noise channel, $\lambda = 1/300$ s, $\mu = 1/120$ s, $E_{\text{Batt}} = 6$ Wh). PRB, physical resource block; CoPoMo, context-aware power consumption model.

9.3. Power efficient real-time applications

Different than the non-real-time applications, real-time applications such as VoIP or video streaming cannot benefit from increasing data rates, as the data that needs to be transferred becomes continuously generated by the codec. Therefore, a continuously available fixed data rate channel needs to be provided by the system. To achieve a constant bit rate, a degradation of the radio channel needs to be compensated by the allocation of additional PRBs.

9.3.1. Trading PRBs for battery lifetime.

As it can be seen from Figure 18 (1), the average number of PRBs that are needed for achieving a given throughput of 500 kbit/s is controllable by the target SNR. For lower values of SNR_T, the average power consumption P_Σ decreases but at the expense of an increasing number of necessary PRBs. If there are unused PRBs available, for example, because the cell is not completely occupied, a battery lifetime enhancement of up to 7 per cent is possible by spending only one additional PRB (cf. Figure 18).

9.3.2. Impact of different carrier frequencies.

On top of this, the battery lifetime can be further enhanced by additional 24 per cent if the UE can handover to the more power efficient 800 MHz LTE band (cf. (2) in Figure 18). However, it is worth noting that the energy-saving potential as well as the most energy efficient proceeding does strongly depend on the actual UE (cf. Section 9.2.3). The knowledge about this relationship and quantitative analyses allow network operators to support a trade-off between the cell capacity in different frequency bands and the average battery lifetime of the particular user device inside a cell.

10. CONCLUSION

The key contribution described in this paper is CoPoMo, a context-aware stochastic power consumption model that enables precise battery lifetime forecasts of LTE devices in realistic scenarios. The following results highlight our research about CoPoMo:

- The application of empirically derived device models is necessary for an accurate battery lifetime forecast (cf. Figures 5 and 14).
- The significant impact of physical layer characteristics such as cell environment and radio channel conditions on UE power consumptions has been demonstrated (cf. Figure 14).
- The application of CoPoMo for concrete forecasts of the context-dependent battery lifetime has been illustrated (cf. Figures 14, 16 and 18).
- The Markovian-based power consumption modelling including the differentiation between different application types is important for the optimal system parameterisation (cf. Figures 16 and 18).
- An example on how the battery lifetime can be greatly enhanced by energy efficient PRB allocation in time and frequency domains was given (cf. Figure 16).

All results have been validated by an independent system simulation. Our future work will extend the generic CoPoMo approach to other wireless communication networks, including LTE Advanced. Beyond that, we are going to perform extensive field trials in public LTE networks for further validation of the CoPoMo.

ACKNOWLEDGEMENT

Part of the work on this paper has been supported by Deutsche Forschungsgemeinschaft (DFG) within the

Collaborative Research Center SFB 876 'Providing Information by Resource-Constrained Analysis', projects A4 and B4.

REFERENCES

1. Müllner R, Ball CF, Boussif M, Lienhart J, Hric P, Winkler H, Kremnitzer K, Kronlachner R. "Enhancing uplink performance in UTRAN LTE networks by load adaptive power control". *European Transactions on Telecommunications* 2010; **21**: 458–468.
2. Kawadia V, Kumar PR. "Power control and clustering in ad hoc networks", In *Proc. 22nd IEEE International Conference on Computer Communications (INFOCOM)*, San Francisco, CA, USA, 2003; 459–469.
3. Jin T, Noubir G, Sheng B. "WiZi-Cloud: application-transparent dual ZigBee-WiFi radios for low power internet access", In *Proc. IEEE International Conference on Computer Communications (INFOCOM)*, Shanghai, China, 2011; 1593–1601.
4. Deruyck M, Joseph W, Martens L. "Power consumption model for macrocell and microcell base stations". *Transactions on Emerging Telecommunications Technologies* accepted 2012.
5. Elayoubi S-E, Saker L, Chahed T. "Optimal control for base station sleep mode in energy efficient radio access networks", In *Proc. IEEE International Conference on Computer Communications (INFOCOM)*, Shanghai, China, 2011; 106–110.
6. Adibi S, Mobasher A, Tofigh T. "LTE networking: extending the reach for sensors in mHealth applications". *Transactions on Emerging Telecommunications Technologies* accepted 2013.
7. Fu H-L, Chen H-C, Lin P, Fang Y. "Energy-efficient reporting mechanisms for multi-type real-time monitoring in Machine-to-Machine communications networks", In *Proc. IEEE International Conference on Computer Communications (INFOCOM)*, Orlando, FL, USA, 2012; 136–144.
8. Ide C, Dusza B, Wietfeld C. "Energy efficient LTE-Based floating car data collection for dynamic traffic forecasts", In *Proc. IEEE International Conference on Communications (ICC)*, Ottawa, Canada, June 2012.
9. Kim GS, Je YH, Kim S. "An adjustable power management for optimal power saving in LTE terminal baseband modem". *IEEE Transactions on Consumer Electronics* 2009; **55**(4): 1847–1853.
10. Bloom L, Eardley R, Geelhoed E, Manahan M, Ranganathan P. "Investigating the relationship between battery life and user acceptance of dynamic, energy-aware interfaces on handhelds", In *Proc. 6th International Conference on Human Computer Interaction with Mobile Devices and Services (MobileHCI)*, Glasgow, Scotland, 2004.
11. Dufkova K, Le Boudec J-Y, Popović M, Bjelica M, Khalili R, Kencl L. "Energy consumption comparison between macro-micro and public femto deployment in a plausible LTE network", In *Proc. 2nd International Conference on Energy-Efficient Computing and Networking (e-energy)*, New York, USA, 2011.
12. Somavat P, Jadhav S, Namboodiri V. "Accounting for the energy consumption of personal computing including portable devices", In *Proc. 1st International Conference on Energy Efficient Computing and Networking (e-energy)*, Passau, Germany, 2010; 141–149.
13. Saleh AB, Bulakci O, Redana S, Raaf B, Hamalainen J. "Evaluating the energy efficiency of LTE-Advanced relay and picocell deployments", In *Proc. IEEE Wireless Communications and Networking Conference (WCNC)*, Paris, France, 2012; 2363–2367.
14. Lauridsen M, Jensen AR, Mogensen P. "Reducing LTE uplink transmission energy by allocating resources", In *Proc. IEEE 74th Vehicular Technology Conference Fall (VTC-Fall)*, San Francisco, CA, USA, 2011.
15. Jensen AR, Lauridsen M, Mogensen P, Sørensen TB, Jensen P. "LTE UE power consumption model for system level energy and performance optimization", In *Proc. IEEE 76th Vehicular Technology Conference Fall (VTC-Fall)*, Quebec City, Canada, 2012.
16. Dusza B, Ide C, Cheng L, Wietfeld C. "An accurate measurement-based power consumption model for LTE uplink transmissions", In *Proc. IEEE INFOCOM (Poster)*, Turin, Italy, 2013.
17. Fowler S, Bhamber RS, Mellouk A. "Analysis of adjustable and fixed DRX mechanism for power saving in LTE/LTE-Advanced", In *Proc. IEEE International Conference on Communications (ICC)*, Ottawa, Canada, 2012.
18. Staudinger J. "Applying switched gain stage concepts to improve efficiency and linearity for mobile CDMA power amplification". *Microwave Journal* 2000; **43**(9): 152–162.
19. LTE physical layer procedures, Sep. 2009. 3GPP TS 36.213, V 9.3.0.
20. UE radio transmission and reception, January 2012. 3GPP TS 36.101, V 9.10.0.
21. Pop V, Jan Bergveld H, Danilov D, Regtien PPL, Notten PHL. *Battery Management Systems: Accurate State-of-Charge Indication for Battery-Powered Applications*. Springer: New-York, 2008.
22. Little JDC. "A Proof for the queuing formula: $L = \lambda W$" 1961; **9**(3): 383–387.
23. Kleinrock L. *Queueing Systems, Vol. 1 - Theory*. John Wiley & Sons, Ltd.: New-York, 1975.
24. Selection procedures for the choice of radio transmission technologies of the UMTS, 1998. 3GPP TR 101 112, V3.2.0.

25. Dusza B, Ide C, Wietfeld C. "Measuring the impact of the mobile radio channel on the energy efficiency of lte user equipments", In *Proc. 21st International Conference on Computer Communication Networks (ICCCN)*, Munich, Germany, 2012.
26. Bulakci O, Redana S, Raaf B, Hamalainen J. "Impact of power control optimization on the system performance of relay based LTE-Advanced heterogeneous networks,". *Journal of Communications and Networks* 2011; **13**(4): 345–359.
27. Boudreau G, Panicker J, Guo N, Chang R, Wang N, Vrzic S. "Interference coordination and cancellation for 4G networks". *IEEE Communications Magazine* April 2009; **47**: 74–81.
28. Calabrese FD, Anas M, Rosa C, Mogensen PE, Pedersen KI. "Performance of a radio resource allocation algorithm for UTRAN LTE uplink". *Proc. 65th IEEE Vehicular Technology Conference Spring* 2007: 2895–2899.
29. Novlan TD, Dhillon HS, Andrewes JG. "Analytical modeling of uplink cellular networks". *IEEE Transactions on Wireless Communications* 2013. Available online at http://arxiv.org/abs/1203.1304.
30. Woelfle G, Hoppe R, Landstorfer FM. "A fast and enhanced ray optical propagation model for indoor and urban scenarios, based on an intelligent preprocessing of the database", In *Proc. 10th IEEE International Symposium on Personal, Indoor and Mobile Radio Communications*, Osaka, Japan, 1999.
31. Physical layer aspects for evolved Universal Terrestrial Radio Access (UTRA), September 2006. 3GPP TR 25.814.
32. Base Station (BS) radio transmission and reception, November 2008. ETSI TS 136 104, V 8.3.0.
33. Holma H, Toskala A. *WCDMA for UMTS - HSPA Evolution and LTE*, 5th ed. John Wiley & Sons, 2010.